Mustansiriyah Journal of Materials Engineering and Sustainability
Volume 01, No. 01, 2025, Pages 13-19
https://mjmes.uomustansiriyah.edu.iq/
Research Article

DOI: https://doi.org/10.31272/p3gq7r62

ISSN: 3079-9899 (Print)
ISSN: 3079-9902 (Online)

Thermal conductivity investigation of titanium dioxide nanoparticles embedded paraffin wax for thermal energy storage applications

Bydaa Jaber Nabhan[1*], Lubna Ghalib[1], Shaukat Ali Mazari[2]

[1]Materials Engineering Department, College of Engineering, Mustansiriyah University, Baghdad, Iraq
[2]Department of Chemical Engineering, Dawood University of Engineering and Technology, Karachi-74800, Pakistan
[*]Email: lubnaghalib81@uomustansiriyah.edu.iq

Article Info

Received	20/04/2025
Revised	14/06/2025
Accepted	14/06/2025
Published	01/07/2025

Abstract

To enhance the efficacy of thermal conversion systems, it is imperative to incorporate them with thermal energy storage mechanisms. Within the extensive selection of essential materials, phase change materials (PCMs) are identified as the top choice for the retention and later liberation of thermal energy, attributable to their notable latent heat of fusion. Generally, PCMs exhibit low thermal conductivity. Incorporating nano additives has been explored to improve the thermal characteristics of PCMs further. In our recent exploration, we augmented the thermal conductivity of paraffin wax using different mass concentration additions (1 wt. %, 3 wt. %, 5 wt. Titanium dioxide (TiO_2) nanoparticles exist at a percentage that is roughly 10 nm in diameter. Researchers have noted that introducing TiO_2 nanoparticles into the paraffin wax matrix affects the temperature at which phase changes occur. Also, the thermal conductivity in the resultant composites indicated a falling tendency as temperature increased, due to the increased surface interfacial thermal resistance between TiO_2 nanoparticles and the wax matrix. A notable enhancement in thermal conductivity, quantified at approximately 10% and 7%, was recorded through the utilisation of spherical and trapezoidal capsules, respectively, at a nanoparticle loading of 5 wt. The atmospheric conditions are 50±5% humidity and the temp is at 15°C.

Keywords: Phase change materials, Thermal conductivity, Titanium dioxide, paraffin wax, nanoparticles.

1. Introduction

Energy storage assumes significant functions in mitigating the excessive demand for energy, facilitating its utilization during peak periods. The thermal energy storage (TES) systems are pivotal in the recovery of heat and substantially enhance the operational efficacy of thermal systems. TES systems consist of contained media capable of absorbing thermal energy (charging mode) and subsequently releasing this stored thermal energy (discharging mode) to address deficiencies in the primary thermal source. Typically, the storage medium comprises a fluid or phase change material. Generally, the thermal conductivity of these TES-based materials is suboptimal, resulting in a protracted charging and discharging rate. The rates of charging and discharging can be augmented through the implementation of heat transfer enhancement techniques [1]. In study, Abhat [2] proposed a valuable classification of materials utilized for thermal energy storage, as illustrated in Fig. 1.

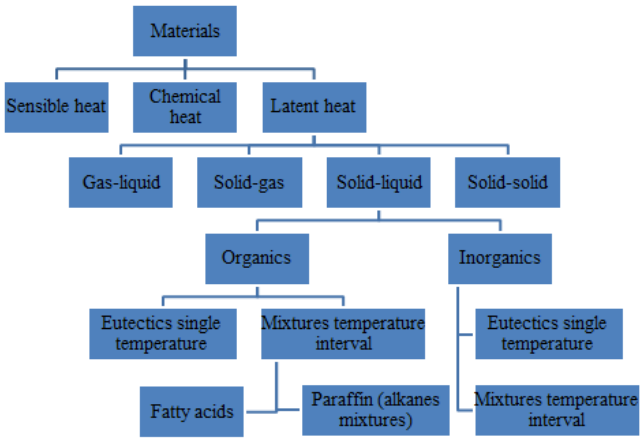

Figure 1. Classification of energy storage materials [2].

Various mechanisms behind enhanced thermal conductivity of nanoparticles have been developed. These mechanisms include Brownian motion-induced microconvection, percolation effects at higher loading of nanoparticles, and interfacial resistance limitations. However, these models are

not capable of representing the wide range of thermal conductivities of several nanoparticles. Numerous scholars have conducted analogous investigations regarding the heat transfer efficacy of nanofluids. For instance, Lee and Choi [3] endeavored to utilize nanofluids in conjunction with miniature heat exchangers to constitute an effective cooling system. Recently, the application of nanofluids has gained traction for boosting heat transfer in phase change materials (PCMs) aimed at energy storage, owing to their impressive capacity for high thermal conductivity. In their study, Xie et al.[4] revealed that Al_2O_3 nanofluid's thermal conductivity was superior to that of the base fluid, and it rose with the enhancement of nanoparticle concentration. The enhanced thermal conductivity ratio diminished in correlation with an increase in pH value, ranging from pH 2.0 to pH 11.5. Additionally, they ascertained that the thermal conductivity of nanofluids was contingent upon particle size, identifying an optimal particle size of 60 nm for the enhancement of thermal conductivity. Khodadadi and Hosseinizadeh [5] examined the phase change phenomena of Cu-H2O nanofluids utilizing a numerical simulation methodology. Nanofluids displayed beneficial thermal energy storage capabilities, with the heat dissipation rate outpacing that of unadulterated water. Wu et al. [6] examined the thermal dynamics of (Al_2O_3-H_2O) nanofluid and concluded that adding 0.2 wt.% Al_2O_3 nanoparticles to water diminished the supercooling by 70.9%. In their study, Ho and Gao [7] examined the significant thermophysical attributes, which included latent heat of fusion, density, dynamic viscosity, and thermal conductivity of n-octadecane PCM that was infused with Al2O3 nanoparticles at 5% and 10% compositions. The emulsification of alumina using a non-ionic surfactant led to this result. The differences regarding melting temperature, freezing temperature, and latent heat of fusion are described in Table 1.

Table 1. Variation in melting, freezing temperatures and latent heat of fusion as a function of different weight % of Al2O3 nanoparticle [7]:

Mass fraction of nanoparticles (wt.%)	Melting temperature (° C)	Freezing temperature (° C)	latent heat of fusion (kJ/kg)
0	26.5	25.1	243.1
5	26	25	225.6
10	26.3	25.3	212.3

Through their investigation, Shin and Banerjee [8] found that high-temperature silica-based nanofluids used for solar thermal energy storage applications had a specific heat capacity enhancement of 14.5%. Qinbo He et al. [9] examined the thermal characteristics of TiO_2 nanoparticles dispersed in a saturated BaCl2 aqueous solution, concluding that the thermal conductivities of nanofluid phase change materials (PCMs) exhibit an increase of 12.76% at a temperature of -5°C, when utilizing a volume fraction of 1.13%.

The investigation by Parameshwaran et al. [10] focused on how well organic esters perform when silver nanoparticles are included, assessing various metrics like latent heat capacity, thermal conductivity, and their potential for heat storage and release. The research results show that the latent heat capacities saw a decrease of (7.88%) while freezing and (8.91%) during melting, with the thermal conductivity of the composite phase change materials (PCMs) rising from (0.284 to 0.765 W/m.K). Mohamed H. Mahmoud and his team [11] explored the improvement of thermal conductivity in paraffin and natural wax composites by using four various high-conductivity additives infused within the wax matrix. The investigation concluded that the copper network (CN) composite with (6%) additives showed a reduction in charging and discharging durations of (26.4%) and (30.3%) respectively, when juxtaposed with pure wax, while also increasing thermal conductivity by a factor of (2.57) related to pure wax. The aim of this investigation is to showcase a strategy designed to elevate the thermal conductivity of paraffin wax as a phase change material (PCM) by using diverse mass ratios of titanium dioxide (TiO_2) nanoparticles.

Theoretical formulation:

Commonly, PCMs that utilize paraffin reveal low thermal conductivity; during the discharge cycle, thermal energy from the PCM in its liquid state is released, resulting in a solid PCM layer forming on the container's walls. The thermal resistance associated with this layer escalates with an increase in thickness, thereby reducing the rate of heat transfer [12]. To counteract this dilemma, nanoparticles, particularly titanium dioxide (TiO_2), have been blended into the PCM, as the small size of these particles contributes to an enhanced specific surface area and surface energy. The measurements are conducted when the requisite number of settings is to be applied:

The case study is characterized by a transient state, given that the temperature varies over time.

2. The inlet of the testing section has been defined as a velocity inlet, with a velocity magnitude of 7 m/sec and a constant temperature for the heat transfer fluid of 76 °C during the charging phase and 12 °C during the discharging phase.

3. The outlet section of the testing apparatus was designated as an outflow boundary, which is intended for use with incompressible flow.

4. The wall of the duct was presumed to be thoroughly insulated, leading to the assumption of an adiabatic condition.

The illustration in Fig. 2 showcases a tangible depiction of the numerical model. The governing conservation equations are formulated as follows [11]:

Continuity equation

$$\nabla \vec{u} = 0 \quad (1)$$

- Momentum equation:

$$\rho_{wf} \cdot \frac{\partial u}{\partial t} = -\nabla P + \mu \nabla^2 \vec{u} \quad (2)$$

Where P: Pressure gradient with velocity fluid (N/m^2).

- Energy equation:

The enthalpy of a material is [11]:

$$H = H_{sensible} + H_{latent} \quad (3)$$

$$\& \quad H_{sensible} = H_{ref} + \int_{T_{ref}}^{T} C_p dT \quad (4)$$

Where: H_{ref}: Reference enthalpy (kJ/kg), T_{ref}: Reference temperature (°C), The latent heat content can be written by latent heat of the material and L:

$$H_{latent} = \beta.L \quad (5)$$

Where β: Liquid fraction can be defined as:

$\beta=0$ if $T \leq Tsolidus$

$\beta=1$ if $T \geq Tliquidus$

$\beta = (T - T_{solidus})/(T_{liquidus} - T_{solidus})$ if $Tsolidus < T < Tliquidus$ (6)

The energy equation is written as [11]:

$$\frac{\partial}{\partial t}(\rho H) + \nabla.(\rho \vec{u} H) = \nabla.(K \nabla T) + S \quad (7)$$

Where S: Represents the dissipation function. This function encompasses the energy that is converted into thermal energy as a result of the fluid shear stress.

The rate of energy storage or release is largely determined by the thermal conductivity, making it an essential trait of phase change materials (PCMs). PCMs are employed for the purpose of thermal energy storage in environments characterized by temperature fluctuations. Consequently, it is essential to ascertain the thermal conductivity of the PCMs in both their solid and liquid phases across the relevant temperature range. Numerous theoretical examinations have been executed to determine the thermal conductivities of the composite materials. The formula utilized for the computation of the thermal conductivities of the composite is [13]:

$$k_C = \varphi_v * k_P + (1 - \varphi_v) * k_f \quad (8)$$

In this scenario k_c, k_p, and k_f illustrate the thermal conductivities of the composite, nanoparticle, and matrix, respectively. The correlation between volume fraction φ_v and weight fraction φ_w is articulated in reference[13]:

$$\varphi_v = (m_P * \rho_c)/(m_c * \rho_p) = \varphi_w * (\rho_c/\rho_p) \quad (9)$$

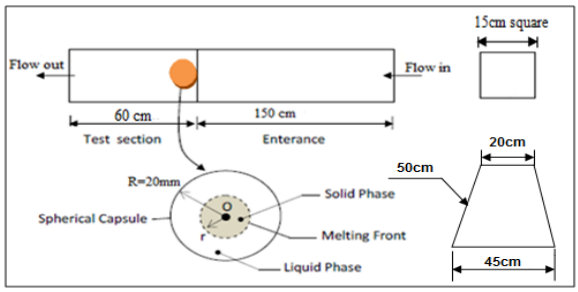

Figure 2. Schematic diagram of the numerical model.

The tabulated mass fraction corresponding to the volume fraction of the samples is presented in Table 2. In Table 3, the attributes of the nanoparticle (TiO_2) alongside the phase change material (PCM) are presented.

Table 2. The wt. % associated with vol. % of the nanoparticle sample at 200C.

wt.%	vol.%
1	2.57
3	2.68
5	2.798

Table 3. The properties of nanoparticle and PCM.

	Density (kg/m^3)	Thermal conductivity (W/m.k)	Specific heat (J/kg.k)	Melting temperature (°C)
TiO_2 (dp=10 nm)	4230	8.4	710	---
PCM (paraffin wax)	785	0.214	2871	62-68

Experimental test rig:

Fig. 3 illustrates the configuration of the experimental test rig. The experimental test rig comprises the essential components depicted schematically in Fig. 4, including the flow unit, which contains refrigerated air and operates via a three-phase electric motor, and the heating unit, which is equipped with three electrical helical heaters (600 Watts each) utilized for elevating the temperature within the test section. The duct section possesses a square cross-sectional area of (15x15) cm^2 and extends to a length of (210 cm), with the test section situated at the terminal (60 cm) of the duct. A total of (120) spherical capsules, each containing (25 g) of phase change material (PCM), have been strategically arranged within the test section. The test rig is insulated with a layer of glass wool.

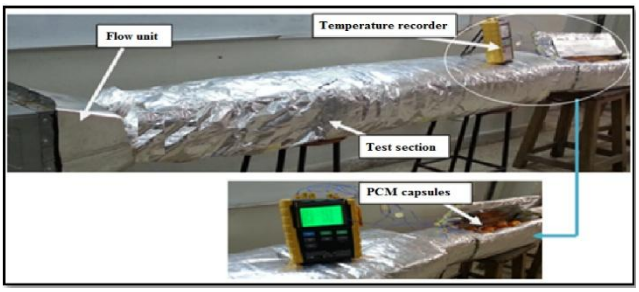

Figure 3. Experimental test rig.

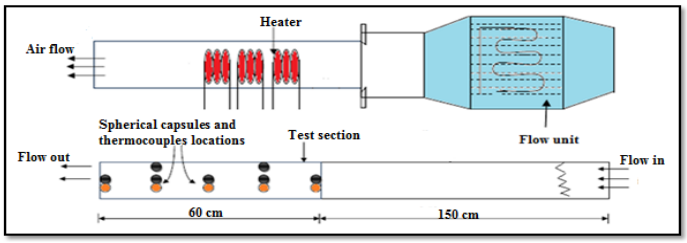

Figure 4. Schematic diagram of the experimental apparatus.

Measurement instrument:

Temperature and air velocity were quantified utilizing specialized measuring instruments. Thermocouples of type T were employed to ascertain the temperatures of phase change materials (PCM) and air at five distinct locations along the axial orientation within the testing apparatus, as recorded through the utilization of digital thermometers. Five uniquely

crafted capsules that contain thermocouples are systematically arranged along the centerline of the testing segment at axial positions of X/L = 0, 0.25, 0.5, 0.75, and 1. A thermal imaging camera, specifically the Ti32, was used to monitor the surface temperature of the test capsules, as represented in Fig. 5.

Figure 5. Thermal camera

A digital vane anemometer was employed to ascertain the mean air velocity at both the inlet and outlet of the specified section.

Results and discussion:

In the current investigation, enhancements in the thermal conductivity of phase change materials (PCM) for thermal energy storage are elucidated, alongside the outcomes of the charging and discharging procedures which are also delineated herein.

Figs 6 and 7 illustrate thermal imagery of PCM and the alterations in thermophysical properties corresponding to varying weight percentages of the nanoparticle TiO_2 at 60°C, following a 15-minute interval. Furthermore, these Figs display three-dimensional representations and the temperature distribution for both spherical and trapezoidal capsules, respectively. One notable aspect is that the melting process accelerates with the growing mass fraction of TiO_2 nanoparticles compared to pure paraffin, owing to the increased surface energy tied to the small scale of the nanoparticles.

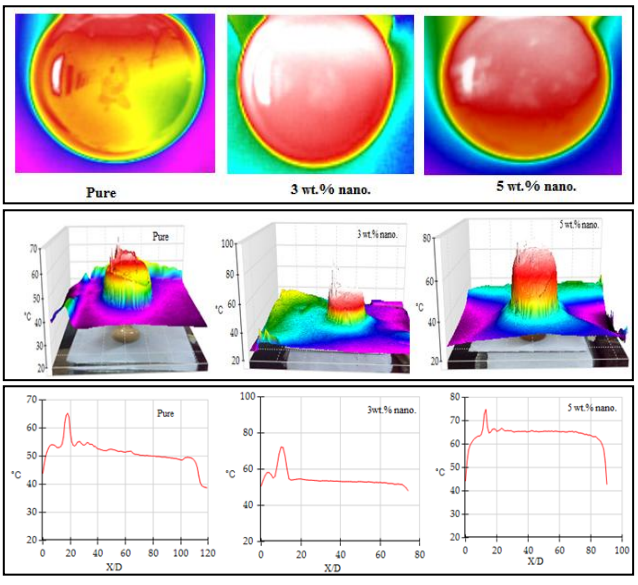

Figure 6. (a) Thermal images for spherical capsules of PCM at different weight% of nanoparticle TiO_2 at 60°C and after15 minute, (b) 3D-IRTM and (c) Temperature distribution.

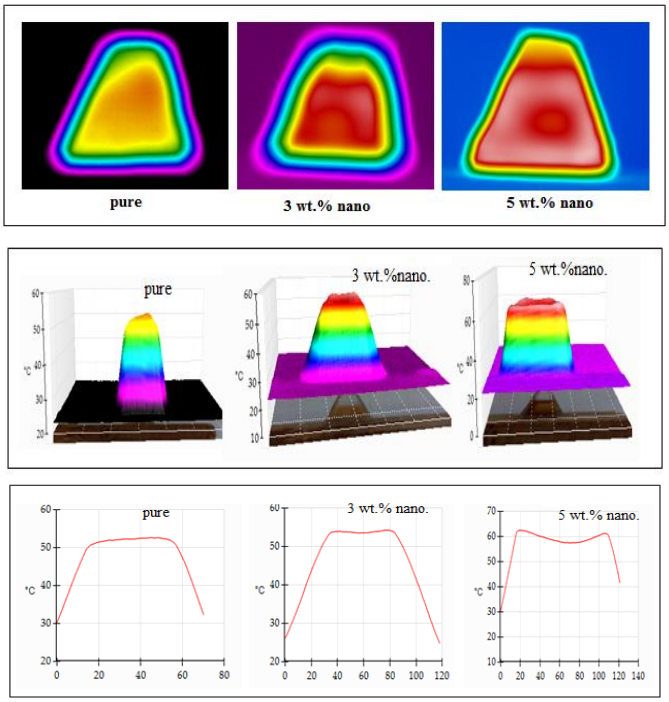

Figure 7. (a) Thermal images for trapezoidal capsules of PCM at different weight% of nanoparticle TiO_2 at 60°C and after15 minute, (b) 3D-IRTM and (c) Temperature distribution.

Figs 8, 9, and 10 showcase the temperature distribution of the Phase Change Material (PCM) along the axial direction of the experimental section at designated ratios of (X/L=0, 0.25, 0.5, 0.75, and 1), with a flow speed recorded at (7m/s). It is evident that during the charging process, at (X/L = 0), the PCM exhibits a more rapid melting rate compared to other locations, as it absorbs the majority of the thermal energy conveyed by the heat transfer fluid; this energy diminishes progressively as it traverses over the capsules indicated throughout the test section, resulting in the final PCM capsules at the terminal section possessing insufficient energy to undergo melting. The heat transfer mechanisms between the PCM and the heat transfer fluid are significantly enhanced and become increasingly effective by (11.5%) for spherical capsules and (10.3%) for trapezoidal capsules upon the introduction of a mass fraction (5 wt. %) of the nanoparticle TiO_2, due to the reduction in thermal resistance.

During the discharge process, a reverse mechanism occurs to facilitate the release of the absorbed energy. It can be observed that the initial capsules solidify at a more rapid pace than the subsequent ones, and the solidification process transpires more swiftly than the melting process, attributable to the diminished thermal resistance of the liquid PCM. The incorporation of various mass fractions of the nanoparticle TiO2 within the PCM promotes the enhancement of the heat transfer process between the PCM and the heat transfer fluid.

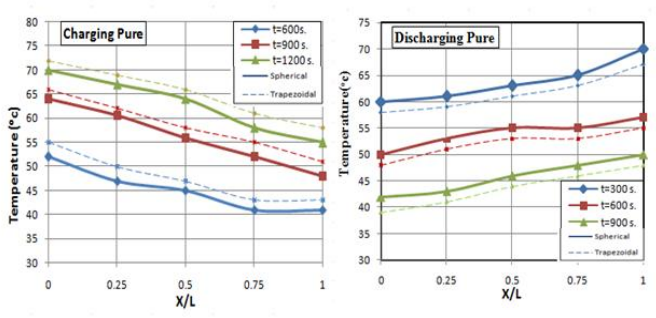

Figure 8. Distribution the temperature of PCM along the axial direction of the test section during charging and discharging processes.

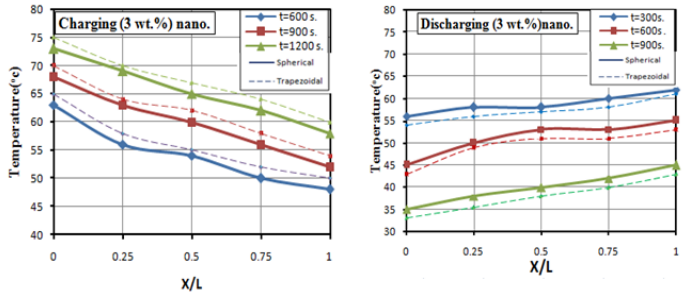

Figure 9. Distribution the temperature of PCM with (3 wt. %) nano. along the axial direction of the test section during charging and discharging processes.

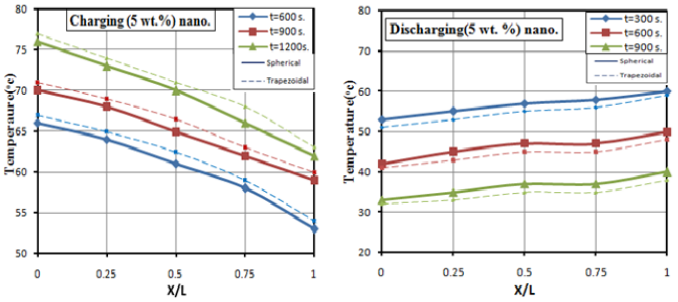

Figure 10. Distribution the temperature of PCM with (5 wt. %) nano. along the axial direction of the test section during charging and discharging processes.

Fig. 11 illustrates the latent heat corresponding to varying mass fractions of TiO_2 nanoparticles. Research indicates that the latent heat of fusion for composite phase change materials (PCMs) falls off as the mass fraction expands. The drop can be ascribed to two significant causes: the first being that the nanoparticles' specific heat capacity is less than that of the PCM, resulting in diminished overall thermal absorptance for the composite PCM. The second factor involves the alteration of the molecular arrangement within the PCM crystals induced by the nanoparticles, which influences the melting capability and subsequently impacts the latent heat of fusion. Therefore, the thermal properties of the system are notably affected [14].

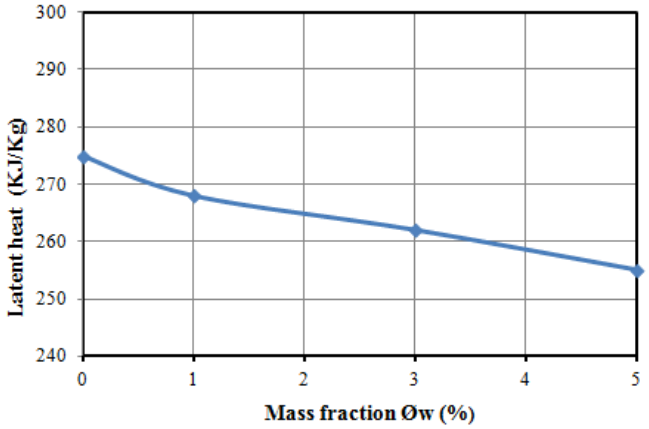

Figure 11. Effect mass fraction of nanoparticles on the latent heat of fusion of composite PCMs.

Fig. 12 illustrates the augmented thermal conductivity (K) as a function of the mass fraction of TiO_2 nanoparticles at three distinct testing temperatures. It is observed that (K) diminishes with rising temperature, while it exhibits an increase with the augmented loading of TiO_2 nanoparticles. Specifically, when the mass fraction is (5 wt. % and T=15°C), the thermal conductivity is enhanced by (10%). Still, the enhancement seen in thermal conductivity might stem from alterations in dynamic viscosity.

As shown in Fig. 12 can be observed that the thermal conductivity decrease with increasing temperature due to the phase transitions in paraffin wax which disrupts phonon transport. At elevated temperatures, titanium dioxide nanoparticles agglomerate, reducing effective conductive pathways.

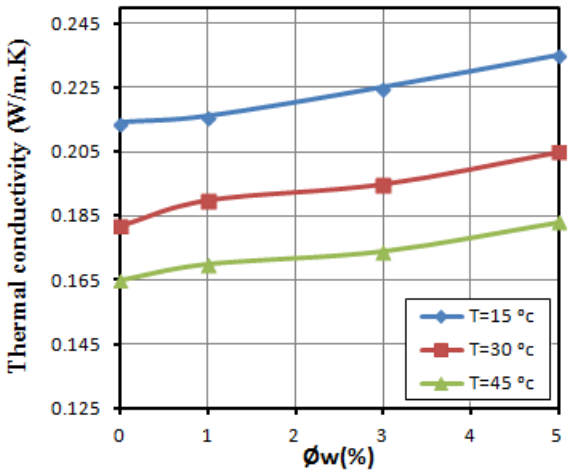

Figure 12. Effect mass fraction of nanoparticles on the thermal conductivity at different temperatures.

Conclusions

In the current investigation, the ensuing conclusions have been derived:

The enhancement of the heat transfer process has been quantified at 11.5% for spherical capsules and 10.3% for trapezoidal capsules, attributed to the incorporation of a mass fraction of 5 wt.% of the nanoparticle TiO_2. The phenomenon of solidification is observed to transpire at a rate that exceeds that of melting, owing to the presence of diminished thermal resistance. The rates of thermal storage and release have been determined to augment by approximately 20% for spherical capsules in comparison to trapezoidal capsules at a temperature of 50°C. Thermal conductivity exhibits a decline with an elevation in temperature; conversely, it demonstrates an increase with a heightened loading of the nanoparticle TiO_2, specifically by 10% at 5 wt.% and at a temperature of 15°C.

Acknowledgements

The authors would like to thank Mustansiriyah University (www.uomustansiriyah.edu.iq) Baghdad – Iraq for its support in the present work.

Abbreviations

Cp: Specific heat at constant pressure (kJ/kg.^{o}C)
D: diameter of capsule (m)
H : Specific enthalpy(kJ/kg)
k: Thermal conductivity (W/m.^{o}C)
L: Length of test section (m)
m:Mass (kg)
P: Static pressure (N/m^2)
u: Velocity (m/s)
∇: gradient.
μ: Dynamic viscosity (N.s/m^2)
φ_v: Particle volume fraction (%vol.)
φ_w: Particle weight fraction (%wt.)
ρ: Density (kg/m^3)

Conflict of interest

The authors declare that there are no conflicts of interest regarding the publication of this manuscript.

Author Contribution Statement

B.J. Nabhan: proposed the research problem.

B.J. Nabhan, L. Ghalib: developed the theory and performed the computations.

L. Ghalib, S.A. Mazari: verified the analytical methods and investigated the data and supervised the findings of this work.

All authors discussed the results and contributed to the final manuscript.

AI Declaration Statement

The authors confirm that the manuscript has been written without the assistance of generative AI or AI-based writing tools.

References

[1] H. H. Al-Kayiem, S. C. Lin, and A. Lukmon, "Review on nanomaterials for thermal energy storage technologies," *Nanoscience & Nanotechnology-Asia,* vol. 3, pp. 60-71, 2013.https://doi.org/10.2174/2211352511311999001 1.

[2] A. Abhat, "Low temperature latent heat thermal energy storage: heat storage materials," *Solar energy,* vol. 30, pp. 313-332, 1983.https://doi.org/10.1016/0038-092X(83)90186-X.

[3] S. Lee and S. U.-S. Choi, "Application of metallic nanoparticle suspensions in advanced cooling systems," in *ASME International Mechanical Engineering Congress and Exposition*, 1996, pp. 227-234.https://doi.org/10.1115/IMECE1996-0161.

[4] H. Xie, J. Wang, T. Xi, Y. Liu, F. Ai, and Q. Wu, "Thermal conductivity enhancement of suspensions containing nanosized alumina particles," *Journal of applied physics,* vol. 91, pp. 4568-4572, 2002.https://doi.org/10.1063/1.1454184.

[5] J. Khodadadi and S. Hosseinizadeh, "Nanoparticle-enhanced phase change materials (NEPCM) with great potential for improved thermal energy storage," *International communications in heat and mass transfer,* vol. 34, pp. 534-543, 2007.https://doi.org/10.1016/j.icheatmasstransfer.2007.02.005.

[6] S. Wu, D. Zhu, X. Li, H. Li, and J. Lei, "Thermal energy storage behavior of Al2O3–H2O nanofluids," *Thermochimica Acta,* vol. 483, pp. 73-77, 2009.https://doi.org/10.1016/j.tca.2008.11.006.

[7] C. J. Ho and J. Gao, "Preparation and thermophysical properties of nanoparticle-in-paraffin emulsion as phase change material," *International Communications in Heat and Mass Transfer,* vol. 36, pp. 467-470, 2009.https://doi.org/10.1016/j.icheatmasstransfer.2009.01.015.

[8] D. Shin and D. Banerjee, "Enhancement of specific heat capacity of high-temperature silica-nanofluids synthesized in alkali chloride salt eutectics for solar thermal-energy storage applications," *International journal of heat and mass transfer,* vol. 54, pp. 1064-1070, 2011.https://doi.org/10.1016/j.ijheatmasstransfer.2010.11.017.

[9] Q. He, S. Wang, M. Tong, and Y. Liu, "Experimental study on thermophysical properties of nanofluids as phase-change material (PCM) in low temperature cool storage," *Energy conversion and management,* vol. 64, pp. 199-205, 2012.https://doi.org/10.1016/j.enconman.2012.04.010.

[10] R. Parameshwaran, R. Jayavel, and S. Kalaiselvam, "Study on thermal properties of organic ester phase-

change material embedded with silver nanoparticles," *Journal of thermal analysis and calorimetry,* vol. 114, pp. 845-858, 2013.https://doi.org/10.1007/s10973-013-3064-9.

[11] M. H. Mahmoud Alhamdo, B. A. Bdaiwi, and A. H. Hasan, "Transient response of different highly conductive PCM composites," in *International Congress on Energy Efficiency and Energy Related Materials (ENEFM2013) Proceedings, Antalya, Turkey, 9-12 October 2013*, 2014, pp. 253-264.https://doi.org/10.1007/978-3-319-05521-3_33.

[12] S. D. Sharma and K. Sagara, "Latent heat storage materials and systems: a review," *International journal of green energy,* vol. 2, pp. 1-56, 2005.https://doi.org/10.1081/GE-200051299.

[13] P. Bhattacharya, S. Saha, A. Yadav, P. Phelan, and R. Prasher, "Brownian dynamics simulation to determine the effective thermal conductivity of nanofluids," *Journal of Applied Physics,* vol. 95, pp. 6492-6494, 2004.https://doi.org/10.1063/1.1736319.

[14] Y. Cai, Q. Wei, F. Huang, and W. Gao, "Preparation and properties studies of halogen-free flame retardant form-stable phase change materials based on paraffin/high density polyethylene composites," *Applied Energy,* vol. 85, pp. 765-775, 2008.https://doi.org/10.1016/j.apenergy.2007.10.017.